Research Article

SOHAG JOURNAL OF SCIENCES

https://doi.org/10.21608/sjsci.2024.252882.1160

Creation of Silver-Gold Alloy Nanoparticles Using *Citrus sinensis* Peel Extract and Their Antibacterial Efficacy

Bahig EL-Deeb[1], Amira Atef[1,*], Khaled Mohamed[2], and Khalid Abd-elrahim[1]

[1]*Botany and Microbiology Department, Faculty of Science, Sohag University, Sohag 82524, Egypt.*
[2]*Chemistry Department, Faculty of Science, Sohag University, Sohag 82524, Egypt.*
[*]*Email: amira.atef@science.sohage.edu.eg*

Received: 3rd December 2023, **Revised:** 25th January 2024, **Accepted:** 10th March 2024
Published online: 5th April 2024

Abstract: The current investigation employed an aqueous waste peel extract of *Citrus sinensis* (Family: *Rutaceae*) to fabricate monometallic (silver (Ag), (gold (Au), and bimetallic silver –gold alloy nanoparticles (Ag: Au alloy NPs). The results proved that pH 8 and 30 ºC are optimal for producing (Ag, Au, and Ag: Au alloy NPs) utilizing peel extract of *Citrus sinensis* as reducing as well as stabilizing agents. The visual investigation of the bio-synthesized (AgNPs, AuNPs, and Ag: Au alloy NPs) indicated that the color shift from colorless to yellow-brown, violet, and purple, respectively. UV-visible spectroscopy has been employed to establish the synthesis of AgNPs, AuNPs, and Ag_1:Au_1 alloy NPs, each with unique characteristics absorbance peaks at 424, 545, and 498 nm, respectively. Ag and Ag: Au alloy NPs exhibited different antibacterial activities against *Pseudomonas aeruginosa* when biosynthesized at different temperatures. The pronounced antibacterial activities were achieved at 30ºC, whereas at high temperatures (60 ºC), they showed a minor effect. Bio-fabricated mono and bimetallic nanoparticles showed that Gram-negative bacteria tend to be more vulnerable because of their cell wall composition. We will try to find out more medical applications of Ag-Au alloy nanoparticles.
Keywords: silver, gold, nanoparticles, plant extracts, green chemistry, biosynthesis, UV-visible spectroscopy, antibacterial activity.

1. Introduction

Nanotechnology is concerned with the comprehension and manipulation of matter at scales between 1 nm and 100 nm. Nanobiotechnology combines the fields of nanotechnology and biology to generate biological and biochemical materials, devices, and systems at the nanoscale. Owing to their high surface-to-volume ratio and very small size (in nanometers), nanoparticles (NPs) are subject to excessive interest because they have superior physical and chemical properties compared to most of the same bulk molecules. Currently, modified or synthesized NPs are extensively used in industrially produced products, such as skin care products, electronics, and textiles. Metallic nanoparticles have been produced via a variety of physical and chemical processes including spray pyrolysis, phase transfer, digestive ripening, and co-reduction of metal reactions [1-2].

The fabrication of monometallic nanoparticles (MNPs) is most frequently performed using chemical methods, among other techniques. However, hazardous chemicals and powerful catalysts, which may have adverse environmental effects, are used in the chemical synthesis approach [3-4]. Biological hazards, however, owing to their significant benefits in terms of safety, cost-effectiveness, and biocompatibility, green synthesis methods have been suggested as environmentally friendly alternatives to physical and chemical methods. These methods use microorganisms, such as bacteria, fungi, and yeast, as reductants [5-6]. Numerous investigations have already been conducted on the biosynthesis of silver nanoparticles with microbes, involving bacteria such as *Pseudomonas aeruginosa* [7], *Bacillus sp*. [8], *actinobacteria-streptomyces sp*. [9], *Bacillus subtilis* [10], and fungi, such as *Fusarium oxysporum* [11], *Fusarium culmorum* [12], *Fusarium solani* [13], *Phoma glomerata* [14], *Alternaria alternata* [15], *Neurospora crassa* [16], *Trichoderma* [17], *Fusarium graminearum*, *Fusarium scirpi* [18]. AuNPs have also been synthesized using microbes such as: *Bacillus subtilis* [19], and *mesophilic bacterium Shewanella algae* [20]. Several studies have used plant extracts as reducers for the green production of Ag and Au NPs have been described [21,22]. According to Ganesan et al., a liquid extract of *Acorus calamus* rhizome was employed as the reducing agent to produce spherical-shaped, 10 nm-sized Au NPs [23,24]. The active involvement of polyphenolic chemicals found in aqueous extracts of *Elaeis guineensis* leaves in the biosynthesis of Au NPs was established by Ahmad et al. [25]. *Curcumin*'s polyphenolic components have also been used to create high-quality AgNPs in aqueous media [26]. Similarly, leaf extracts from three other plants, *P. urinaria*, *Pouzolzia zeylanica, and Scoparia dulcis*, have recently been used to generate Ag NPs [27].

However, few studies have been conducted on the preparation of bimetallic particles using plant extracts [28]. The leaf broth of *Azadirachta indica* has been used to produce bimetallic Au-Ag NPs [29]. Using *Gloriosa superba* leaf extracts, spherical-shaped Au-Ag NPs with 20 nm in size were created, as reported by Gopinath et al. [30]. Leaf extracts of fenugreek, coriander, and soybean were used as reducing agents to produce three distinct types of Au-Ag bimetallic NPs [31].

Sharma et al. produced Au-Ag NPs using a liquid extract of clove buds [32]. Owing to their exceptional optical, resonance, and chemical qualities, silver and gold nanoparticles offer unique physicochemical features that have been extensively explored for a wide range of applications. Simply because of the monometallic elements' synergistic effects, it has been found that the activities of Ag-AuNPs, or silver-gold alloy nanoparticles, are enhanced [33- 35]. Ag-Au alloy (NPs) may be less toxic than AgNPs [36] and thus more biocompatible for medical purposes because they have a single surface plasmon resonance (SPR) band that is situated midpoint between its monometallic SPR band. Ag, Au, and Au: Ag alloy NPs have a variety of uses, including catalysis [37], antimicrobials, and photothermal action [38,39]. Environmental toxin detectors [40] Biofilm control [41]. This work aimed to synthesize gold, silver, and their bimetallic nanoparticles in an environmentally acceptable approach using an extract of orange peel (*Citrus sinensis*; Family: *Rutaceae*). Optimization factors, including the bulk materials' Au^{+3}, Ag^{+}, pH, temperature, and plant extract quantity, were studied. An ultraviolet-visible spectrophotometer (UV-vis) was utilized to characterize Ag, Au, and three different molar ratios of Ag: Au alloy (NPs). Moreover, antibacterial was studied. Ag: Au alloy nanoparticles were formed within one container. Individually, the raw materials' Ag^{+}/Au^{+3} molar ratios have been adjusted to 1: 3, 1: 1, and 3: 1. $HAuCl_4$ and $AgNO_3$ were present in concentrations of 1 mM for each. Stock solution's Ag^{+}/Au^{+3} molar ratio was added, 2 mL of orange peel extract and then 18 mL deionized water was mixed in a little glass bottle. Until there was no longer any color change, the synthesis system was continuously stirred. The solution shifted from colorless to reddish-brown and purple after 4 hours, indicating the formation of Ag: Au alloy nanoparticles which were verified using UV spectroscopy.

2. Materials and methods

2.1. Materials

Tetrachloroauric (III) acid ($HAuCl_4$) and silver nitrate ($AgNO_3$) have been obtained from Sigma Aldrich Company, Oxoid-England along with all other chemicals and media. Deionized water was used throughout the tests. Orange was purchased from a local market. The orange peels were removed and diced into small pieces. Using an electric blender, the plant parts were ground into powder after being hot air oven-dried for one day at 40 °C. The dried (powdered) samples were then stored at room temperature in a glass container for subsequent use.

2.2. Plant Extract Preparation

To obtain the aqueous orange peel extract, 5 g of the fine powder orange peel was mixed with 100 mL of deionized water and heated at 70 ºC for 1 hour. with continuous stirring. After filtering utilizing the filter paper of Whatman No. 1, the extract was centrifuged for 10 minutes at 4000 rpm. Finally, supernatant was obtained and used without further purification as reported by Ganaie et al., 2016 [8].

2.3. Biosynthesis of AgNPs and AuNPs

Silver and gold nanoparticles were synthesized as described by Elemike et al., 2019 [42]. In a small glass container, 1 mM of $AgNO_3$ or $HauCL_4$, 2 mL orange peel-extract solution, and 18 mL deionized water have been mixed to produce AgNPs or AuNPs. Using a magnetic stirrer, the solution was steadily agitated until the color stopped changing. The solution turned from colorless to yellow after 4 hours, indicating that Ag^{+} had been reduced to Ag^{0} so AgNPs were synthesized or $Au3^{+}$ to Au^{0} reduction resulting in the production of AuNPs. Using UV-Vis spectroscopy, the formation of AgNPs and AuNPs was verified.

2.4. bio fabrication of silver-gold alloy nanoparticles

Silver-gold BNPs were fabricated as described by Shah et al., 2015 [40]. By coupling the reduction of $AuCl_4$ and $AgNO_3$ Ag: Au alloy nanoparticles were formed within one container. Individually, the raw materials' Ag^{+}/Au^{+3} molar ratios have been adjusted to 1: 3, 1: 1, and 3: 1. $HAuCl_4$ and $AgNO_3$ were present in concentrations of 1 mM for each. Stock solution's Ag^{+}/Au^{+3} molar ratio was added, 2 mL of orange peel extract, and then 18 mL deionized water was mixed in a little glass bottle. Until there was no longer any color change, the synthesis system was continuously stirred. The solution shifted from colorless to reddish-brown and purple after 4 hours,indicating the formation of Ag: Au alloy nanoparticles which were verified using UV spectroscopy.

2.5. Optimization parameters used to control synthesis of AgNPs, AuNPs, and Ag: Au alloy NPs

Synthesis of Ag, Au, and Ag: Au alloy NPs is a crucial process that is dependent on several parameters, including the quantity of orange peel -extract, concentration of silver nitrate salt, hydrochloroauric acid salt, temperature, and pH. Various parameters that play key roles in the biosynthesis of monometallic, and bimetallic nanoparticles were briefly described. Such parameters have been improved to produce more stable nanoparticles for the study of specific activities**.**

2.6. Characterization of AgNPs, AuNPs, and Ag: Au alloy NPs

ultraviolet spectroscopy was carried out on a JascoV 7770 UV-Vis spectrophotometer (Japan) in quartz cuvettes. Nine ml of water containing After the reaction, one milliliter of the bio-fabricated NPs was collected and utilized as the sample for measurement.

2.7. Antibacterial activity of biosynthesized AgNPs, AuNPs, and Ag: Au alloy nanoparticles

AgNPs, AuNPs, and Ag: Au alloy NPs were tested for antibacterial activity by employing the disk diffusion approach. according to Ballester-Costa et al., 2017, against *Pseudomonas aeruginosa* and *B. cereus*, a strain of pathogenic bacteria that was freshly cultivated in nutrient broth for 24 h before being inoculated on nutrient agar. the filter paper, Whatman No. 1, was punched into discs with a paper cutter and subsequently placed in a foil packet for sterilization using an autoclave. Discs (5 mm) were loaded with the required concentration of Ag, Au, and Ag: Au alloy NPs. Orange peel -extract was used as negative control while Antibiotics used as positive control. After the incubation period for twenty-four hours at 37°C, the diameter (mm) of the

inhibitory zones surrounding each disc was measured to determine the presence of antibacterial activity.

3. Results and Discussion:

3.1. Visual analysis and biosynthesis of Ag, Au, and Ag-Au alloy nanoparticles

This paper demonstrates the use of orange peel extract in the production of AgNPs, AuNPs, and Ag-Au alloy NPs. Visual observation of the orange peel-extract incubation with $AgNO_3$ at 30°C for 4 hrs in the dark revealed an alteration in color from colorless to (pale yellow, and pale or dark brown), demonstrating the synthesis of yellow-brown elemental Ag^0, which is the characteristic for AgNPs formation, also in case of $HAuCL_4$ a color turn from colorless to light and deep purple was showed indicating the development of purple-colored elemental Au^0, that is indicative of the synthesis of AuNPs.

The creation of Ag: Au alloy NP is indicated by the purple or reddish-brown color when three varied molar ratios of $AgNO_3$/$HAuCL_4$ are used. Color variations in colloidal Ag-Au alloys have previously been mentioned, including brown, deep brown, and purple colors [15, 22], (**Figs. 1a - 1e**). Shift in color resulting from the activation of surface plasmon oscillations in Ag, Au, and Ag-Au alloy NPs provides a suitable spectroscopic indicator for their production, however, the absence of color change has been established in $AgNO_3$ and $HAuCL_4$ solution as negative controls. (**Figs.1a - 1e**) Control reactions without the addition of orange peel-extract revealed no modification in color, indicating that orange peel-extract is required for the reduction of Ag+, Au^{+3}, and Ag^{+}\Au^{+3} as well as nanoparticle formation. Color differences are thought to be due to the configuration of the phytochemical (bio-reductants and bio-capping) agents responsible for the production of Ag, Au, and Ag: Au alloy NPs, which affect their dimensions, form, and optical characteristics [15, 22].

3.2. UV-Visible spectroscopy analysis of Ag, Au, and Ag: Au alloy NPs fabricated at different temperature

Ultraviolet-visible spectroscopy provides a reliable and effective preliminary approach for characterizing NPs. It was also used to investigate the synthesis, and stability of AgNPs, AuNPs, and Ag: Au alloys. [27,28]. The Ag and Au nanoparticles displayed an SPR (surface plasmon resonance) band due to the collective vibration of metal along with free band electron conduction [35].

The physical properties of nanoparticles, including the composition, shape, and synthesis matrix, are key factors that influence the SPR band intensity [40]. Spectral analysis studies of Ag, Au, and Ag- Au alloy nanoparticles show an absorption peak scanned from 200-800 nm. The UV-visible spectra of the extract, Au, Ag, and Ag: Au alloy NPs are displayed in (nm. The UV-visible spectra of the extract, Au, Ag, and Ag: Au alloy NPs are displayed in (**Figs. 1a -1e**), along with the typical SPR centered at 424 nm for AgNPs, 545 nm for AuNPs, 467 nm for Ag_3:Au_1, 498 nm for Ag_1:Au_1, and 520 nm for Ag_1:Au_3 alloy NPs. The Ultraviolet-visible spectrum of orange peel-extract, AuNPs, AgNPs, and Ag-Au NPs alloys at 30 °C are shown in (**Fig. 1c**). Ultraviolet-visible spectra of Ag and Au NPs produced at 10 °C (**Fig. 1a**) showed surface plasmon bands with centers at 439 nm for AgNPs and 547 nm for AuNPs, (445, 526 and 530 nm) for the Ag_3:Au_1, Ag_1:$Au_1$and Ag_1:Au_3 alloy NPs , respectively. When a single peak appeared by UV scan, alloys of Ag and Au NPs have produced not just a chemical interaction of two separate metals, but by the orange peel-extracts, whereas producing two peak curves corresponding to Ag and Au NPs [15, 21]. Various papers have indicated that the peaks of AgNPs emerge in this region, although the precise peak position relies on many variables such as dimension, shape, and substance composition, as well as the local environment [43,44].

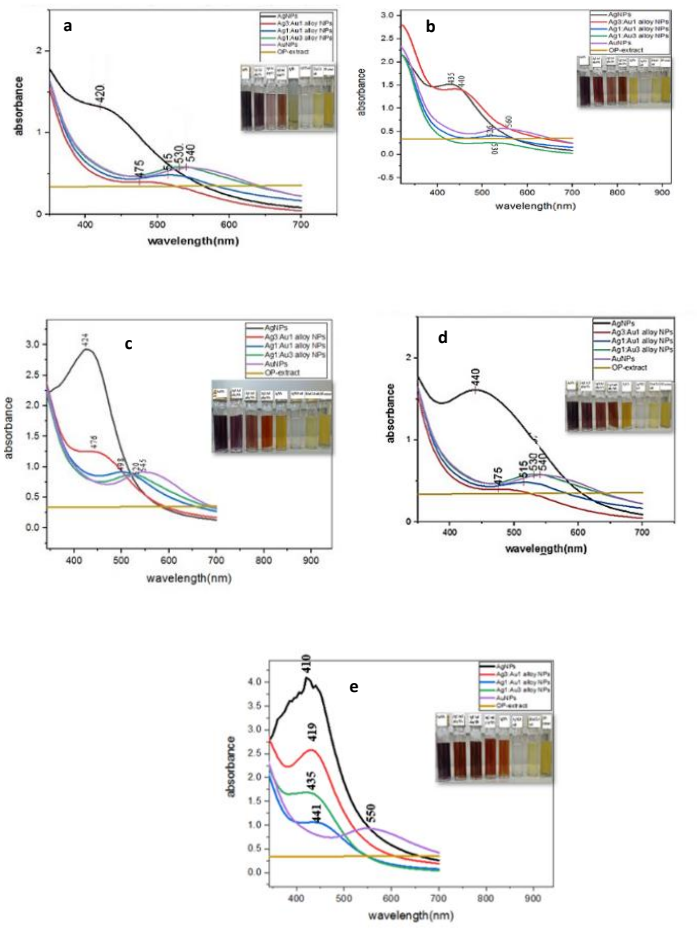

Fig. 1: UV-spectrum and visual analysis of the different temperature effects where A) is 10 °C, B) is 20 °C, C) is 30 °C , D) is 40°C, and E) is 60 °C on the biosynthesis of AgNPs, AuNPs, Ag_3: Au_1, Ag_1: Au_1, Ag_1: Au_3 alloy NPs, and orange peel-extract at (pH=8).

3.3. Antibacterial activity of biosynthesized silver, gold, and silver-gold alloy nanoparticle

The use of biosynthesized nanoparticles in a wide variety of biomedical settings is growing [45]. **Tables (1& 2)** display the outcomes of testing nanoparticles, orange peel extract, and antibiotic reference (cefotaxime) for antibacterial activities. At 150µL, the biosynthesized AgNPs, AuNPs, Ag_3:Au_1, Ag_1:Au_1, and Ag_1:Au_3 alloy NPs showed substantial antibacterial efficacy against gram-positive (*Bacillus cereus*) and gram-negative (*Pseudomonas aeruginosa*) bacterial strains (Muti- Drug Resistant Bacteria, Isolated from Sohag University Hospital). The potency of nanoparticles against gram-positive and gram-

negative bacteria was evaluated after fabrication under optimized conditions temperature, This study confirmed that there is no antibacterial activity with orange peel extract and an antibiotic against tested bacterial strains.

At different temperatures, AgNPs showed inhibition zones against *B. cereus* in the range of 8-21 mm, while the produced AuNPs at 20, and 30 ºC showed inhibition zones of 6, and 12 mm, respectively, however, produced AuNPs at 10,40 and 60 ºC do not affect bacterial growth Under similar conditions, Ag: Au alloy NPs of varying molar ratios (A_3:Au_1, Ag_1:Au_1, and Ag_1:Au_3) showed varying inhibition zones against *B. cereus* 9.5-16.5 mm, 14-28 mm, and 10-15.5 mm, respectively. (**Fig. 2 a-e**). When biosynthesized monometallic and bimetallic nanoparticles at different temperatures were tested against Gram-negative bacteria (*Pseudomonas aeruginosa*), biosynthesized nanoparticles exhibited inhibition zones of 0-30 mm for AgNPs, 0-20 mm for Ag_3:Au_1, 0 - 38mm for Ag_1:Au_1 alloy NPs, 0-13mm for Ag_1:Au_3 alloy NPs and 0-8mm for AuNPs (**Fig. 3 a- e**). The largest inhibition zones (21 mm , 19 mm, 28 mm, 15.5 mm, and 12mm) were recorded for the AgNps, Ag_3:Au_1, Ag_1:Au_1, Ag_1:Au_3 alloys, and AuNPs, respectively, at 30 °C against *B. cereus* (**Fig. 2,c**), moreover, (30 mm, 20 mm, 38 mm, 13 mm, and 8 mm) were recorded for the AgNps, Ag_3:Au_1, Ag_1:Au_1 Ag_1:Au_3 alloyNPs, and AuNPs, respectively, at 30 ºC (**Fig. 3c**) against *Pseudomonas aeruginosa*. Our finding also agrees with the research done by (**Samari, et al. 2018**) [46] who demonstrated that biosynthesized silver nanoparticles were stable at room temperature. Also, Jalab *et al.* 2021 [47] reported that the optimum temperature for AgNPs synthesis was 30 ºC. Whereas (Mittal *et al.* 2013) [48] reported that 30◦C was found to be optimum for gold nanoparticle synthesis. in comparison with Au and Ag NPs alone. These results are in agreement with the results obtained by Tabrizi et al., 2012 [35], who concluded that the enhanced antibacterial activity of Ag_1:Au_1 alloy may be attributed to the combined impact of Ag and Au ions within the nanoparticles [40].

Furthermore, Ag_1:Au_1 alloy was the strongest antibacterial among the Ag: Au alloys nanoparticles (**Figs. 2c**). These finding showed that *P. aeruginosa* (Gram-negative) bacteria were found to be more vulnerable to AgNPs, AuNPs, and Ag-Au bimetallic alloy nanoparticles than *B. cereus* (Gram positive) bacteria. Potentially because of differences in the composition of respective cell wall membranes. Compared to *B. cereus*, *P. aeruginosa* has a thin peptidoglycan layer in its cell wall [7, 10].

In comparison to the other alloy molar ratios, Ag_1:Au_1 alloy NPs exhibited the strongest antibacterial impact, as evidenced by the diameter of the inhibition zones, which were 28 mm against *B. cereus* and 38 mm against *Pseudomonas aeruginosa*. The dual effect of AuNPs and AgNPs that can effortlessly participate in attacking the cell membrane of the microorganism [35] may explain why the antibacterial action of the Ag-Au alloy nanoparticles was more potent than that of the single metal nanoparticles (AgNPs and AuNPs) [44]. The inhibition zone of orange peel extract, silver, gold, as well as silver-gold BMNPs against *Pseudomonas aeruginosa* and *B. cereus* is illustrated in (**Figs. 2 and 3**).

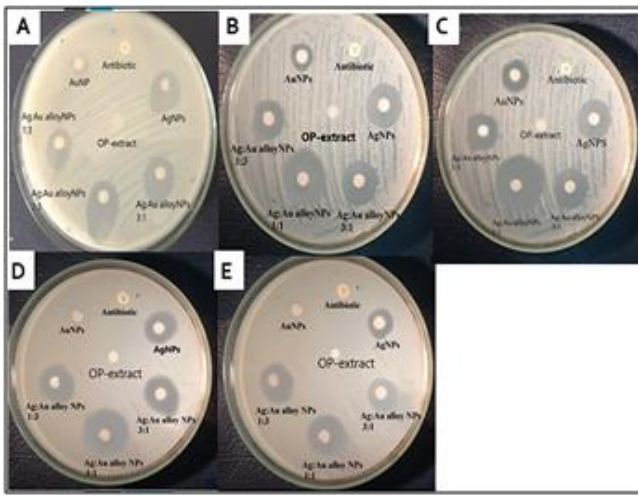

Fig. 2: antibacterial activity of AgNPs, AuNPs, and Ag: Au alloy nanoparticles fabricated at differern temperature where (a) at 10 ºC, (b) at 20ºC, (c) at 30ºc,(d) at 40ºc, and (e) at 60ºC at (pH=8) *against B.cereus*.

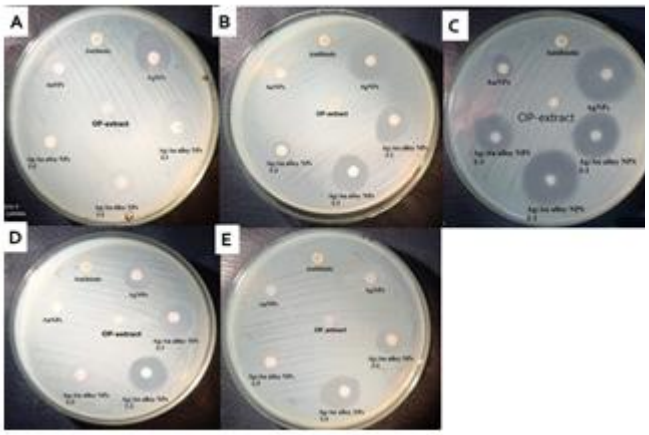

Fig. 3: antibacterial activity of AgNPs, AuNPs, and Ag: Au alloy nanoparticles fabricated at differern temperature where (a) at 10 ºC, (b) at 20ºC, (c) at 30ºc,(d) at 40ºc,and (e) at 60ºC at (pH=8) *against pseudomonas aeruginosa.*

4. Conclusion

An easy, eco-friendly, and economical strategy for the biosynthesis of monometallic Au, Ag, and bimetallic Au–Ag alloy NP catalysts using aqueous extract of orange peel extract as a reducing and stabilizing agent. The physicochemical conditions were optimized for the synthesis of NPs. The biosynthesized monometallic and bimetallic alloy NP were characterized by Ultraviolet-visible spectrum.

The present work provides the optimized conditions for the synthesis of bimetallic Au–Ag alloy NP with high stability and excellent antibacterial activities against pathogenic bacteria gram-positive (*B. cereus*) and gram-negative (*Pseudomonas aeruginosa*) and compared to the monometallic NP. Biosynthesized mono and bimetallic nanoparticles showed that Gram-negative bacteria

(*Pseudomonas aeruginosa*) tend to be more vulnerable because of their cell wall composition.

Table 1: Sizes of the inhibition zones (mm) of AgNPs,AuNPs, and Ag_Au alloy NPs produced under different temperatures conditions against *B. cereus*.

	Pseudomonas aeruginosa				
	Inhibition zone mm				
	T=10°c	**T=20°c**	**T=30°c**	**T=40°c**	**T=60°c**
Orange peel-extract	-	-	-	-	-
Antibiotic	-	-	-	-	-
AgNPs	**14mm**	**16mm**	**30mm**	**8mm**	-
Ag_3:Au_1 alloy NPs	-	**13mm**	**20mm**	**11mm**	**9.5mm**
Ag_1:Au_1 alloy NPs	-	**15.5 mm**	**38mm**	**15mm**	**12mm**
Ag_1:Au_3 alloy NPs	-	**6mm**	**13mm**	-	-
AuNPs	-	-	**8mm**	-	**5.5mm**

Table 2: Sizes of the inhibition zones (mm) of AgNPs, AuNPs, and Ag:Au alloy NPs produced under different temperatures conditions against *Pseudomonas aeruginosa*.

	Bacillus cereus				
	Inhibition zone (mm)				
	T=10°c	T=20°c	T=30°c	T=40°c	T=60°c
Orange peel-extract	-	-	-	-	-
Antibiotic	-	-	-	-	-
AgNPs	13mm	18mm	21mm	10.5mm	8mm
Ag_3:Au_1 alloy NPs	14mm	16.5mm	19mm	13mm	9.5mm
Ag_1:Au_1 alloy NPs	18mm	19.5 mm	28mm	17mm	14mm
Ag_1:Au_3 alloy NPs	10mm	13mm	15.5mm	14mm	11.5mm
AuNPs	-	6mm	12mm	-	-

CRediT authorship contribution statement:

Conceptualization, Bahig El-Deep. and Khalid AbdelRahim.; methodology, Amira Atef.; software, Khaled Mohamed.; validation, Bahig El-Deep., Khaled Mohamed. and Khalid AbdelRahim.; formal analysis, Khalid AbdelRahim; investigation, Amira Atef.; resources, Amira Atef.; data curation, Khaled Mohamed.; writing—original draft preparation, Amira Atef.; writing—review and editing, Bahig El-Deep.; visualization, Khalid AbdelRahim.; supervision, Bahig El-Deep.; project administration, Bahig El-Deep.; funding acquisition, Bahig El-Deep. All authors have read and agreed to the published version of the manuscript."

Data availability statement

The data used to support the findings of this study are available from the corresponding author upon request.

Declaration of competing interest

The authors declare that they have no known competing financial interests or personal relationships that could have appeared to influence the work reported in this paper.

References

[1] N. Kumar, F. Alam and V. Dutta, *Journal of Alloys and Compounds* 585 (2014) 312–317.

[2] N. Tsibakhashvili, T. Kalabegishvili, V. Gabunia, E .Gintury, N.Kuchava, N.Bagdavadze, *Nano Studies*.2(2012) 179-182.

[3] Q. Zhang, J.Y. Lee, J. Yang, , C. Boothroyd, & J. .Zhang, *Nanotechnology*, 18(24) (2007), 245-605.

[4] P. Quaresma, L. Soares,.A. Contar, I. Miranda, P..Osório, A..Carvalho & E. Pereira, *Green Chemistry*, 11(11) (2009). 1889-1893.

[5] Konishi, Y., Ohno, K., Saitoh, N., Nomura, T., Nagamine, S., Hishida, H., ... & Uruga, T, 128(3) (2007). 648-653.

[6] S. Pugazhendhi, E. Kirubha, P.K.. Palanisamy, & R. Gopalakrishnan, *Applied Surface Science*, 357, (2015) 1801-1808.

[7] Y. Konishi, K. Ohno, N. Saitoh, T. Nomura, S. Nagamine, H. Hishida, & T. Uruga, *Journal of biotechnology*, 128(3) (2007) 648-653.

[8] S.U. Ganaie, T., Abbasi, & S.A. Abbasi, *Journal of Experimental Nanoscience* 11(6) (2016) 395-417.

[9] S.D. Deshmukh, SD. Deshmukh, A.K. Gade, M.K. J. Rai, *BioNanoScience*. 6(2012); 90-94.

[10] N. Pugazhenthiran, S. Anandan, G.Kathiravan, N. Kannaian ,U. Prakash, S. Crawford, *Journal of Nanoparticle Research* 11 (2009) 1811-1815.

[11] A. Ahmad, P. Mukherjee, S. Senapati, D. Mandal, M.I. Khan, R. Kumar, *Colloids and Surfaces B: Biointerfaces | Journal* 28 (2003) 313-318.

[12] M. Bawaskar, S. Gaikwad, A. Ingle, D. Rathod, A. Gade, N. Duran, *Current Nanoscience*., 6 (2010); 376-380.

[13] A. Ingle, M. Rai, A. Gade, M. Bawaskar. *Journal of Nanoparticle Research* 11 (2009) 2079-2085.

[14] S.S. Birla, V.V. Tiwari, A.K. Gade, A.P. Ingle, A.P. Yadav, M.K. Rai. *Applied Microbiology and Biotechnology* 48(2009); 173-179.

[15] M. Gajbhiye, J. Kesharwani, A. Ingle, A. Gade, M. Rai. *Nanomed* 5 (2009) 382-386.

[16] E. Castro-Longoria, A.R. Vilchis-Nestor, M. Avalos-Borja *Colloids and Surfaces B: Biointerfaces | Journal* 83(2011) 42-48.

[17] K. Vahabi, G. Mansoori, S. Karimi, *Journal of Nanoscience and Nanotechnology* 1 (2011) 65-79.

[18] S.C. Gaikwad, S.S. Birla, A.P. Ingle, A.K. Gade, P.D. Marcato, M. Rai, & N. Duran, *Journal of the Brazilian Chemical Society* 24(2013) 1974-1982.

[19] T. Beveridge, R.J. Murray Bacteriol, *Journal of bacteriology* 141 (1980) 876–887.

[20] Y. Konishi, K. Ohno, N. Saitoh, T. Nomura, S. Nagamine, *Transactions of the Materials Research Society of Japan* 29 (2004) 2341–2343.
[21] K. Sneha, M. Sathishkumar, J. Mao, I. Kwak, Y.-S. Yun, *Chemical Engineering Journal* 162(2010) 989–996.
[22] R Gangula, L. Podila, C. Karanam, C. Janardhana, A.M. Rao, Langmuir 27(24) (2011) 15268-15274.
[23] M. Ali, T. Ahmed, W. Wu, A. Hossain, R. Hafeez, M. Islam Masum, Y. Wang, Q. An, G. Sun, B. Li, Nanomaterials 10 (6) (2020) 1146.
[24] R. Ganesan, H.G. Prabu, Arabian Journal of Chemistry 12 (2019) 2166–2174.
[25] T. Ahmad, M.A. Bustam, M. Irfan, M. Moniruzzaman, H.M.A. Asghar, S. Bhattacharjee, Applied Biochemistry and Biotechnology 66 (2019) 698–708.
[26] A. Gupta, S.M. Briffa, S. Swingler, H. Gibson, V.; Kannappan, G. Adamus, M. Kowalczuk, C.; Martin, I. Radecka, Biomacromolecules, 2020, 21, 1802–1811.
[27] D.H. Nguyen, J.S. Lee, K.D. Park, Y.C. Ching, X.T. Nguyen, V. Phan, T.T. Hoang Thi, Nanomaterials., 10 (2020) 542.
[28] J.O. Unuofin, A.O. Oladipo, T.A. Msagati, S.L. Lebelo, S. Meddows-Taylor, G.K. More, Arabian Journal of Chemistry 13 (2020) 6639–6648.
[29] S.S. Shankar, A. Rai, A. Ahmad, M. Sastry, Journal of Colloid and Interface Science 275 (2004) 496–502.
[30] K. Gopinath, S. Kumaraguru, K. Bhakyaraj, S. Mohan, K.S. Venkatesh, M. Esakkirajan, P. Kaleeswarran, N.S. Alharbi, S. Kadaikunnan, M. Govindarajan, et al. Microbial Pathogenesis., 101(2016); 1–11.
[31] D. Alti, M.V. Rao, D.N. Rao, R. Maurya, S.K. Kalangi. ACS Omega., 5 (2020);16238–16245.
[32] C. Sharma, S. Ansari, M.S. Ansari, S.P. Satsangee, M. Srivastava, Materials Science and Engineering: C., 116 (2020); 111-153.
[33] S.K. Bhanja, S.K. Samanta, B. Mondal, J S. ana, J. Ray, A. Pandey, T. Tripathy, Environmental Nanotechnology, Monitoring & Management., 14(2020);100-341.
[34] S. M. Roopan, T. V. Surendra, G. Elango, & S. H. S. Kumar, Applied microbiology and biotechnology., 98 (2014);5289-5300.
[35] N.S. Tabrizi, M. Tazikeh, & N. Shahgholi, *International Journal of Green Nanotechnology* 4(4) (2012) 489-494.
[36] T.B. Nguyen, T.D. Nguyen, T.D. Tran, & T.H.N. Thi, *Journal of Cluster Science* 26(5) (2015) 1787-1799.
[37] C. Fasciani, M.J. Silvero, M.A. Anghel, G.A. Arguello, M.C. Becerra, & J.C. Scaiano, (2014). *Journal of the American Chemical Society* 136(50) (2014) 17394-17397.
[38] S. Yallappa, J. Manjanna, & B.L. Dhananjaya, *Spectrochimica Acta Part A: Molecular and Biomolecular Spectroscopy* 137 (2015) 236-243.
[39] S. Shankar, L. Jaiswal, R.S.L. Aparna, & R.G.S.V. Prasad, *Materials Letters* 137(2014) 75-78.
[40] A. Shah, S.B. Khan, A.M. Asiri, H. Hussain, C. Han, R. Qureshi, & H.B. Kraatz, *Journal of Applied Electrochemistry* 45(2015) 463-472.
[41] G.R. Salunke, S. Ghosh, R.J. Santosh Kumar, S. Khade, P. Vashisth, T. Kale, & B.A. Chopade, *International journal of nanomedicine* (2014) 2635-2653.
[42] C. Ballester-Costa, E. Sendra, , J. Fernández-López, J. A. Pérez-Álvarez & M. Viuda-Martos. Foods, 6(8) (2017), 59.
[43] S.V. Chinni, S.C. Gopinath, P. Anbu, N.K. Fuloria, S. Fuloria, P. Mariappan, & S. Samuggam, *Crystals* 11(2) (2021); 97.
[44] E.A. Adebayo, J.B. Ibikunle, A.M. Oke, A. Lateef, M.A. Azeez, A.O. Oluwatoyin, & A.S. Hakeem, *Advanced Material Science* 58(1) (2019) 313-326.
[45] M. El-Khadragy, E. M. Alolayan, D. M. Metwally, M. F. S. El-Din, S.S. Alobud, N.I. Alsultan, & A.E. Abdel Moneim, *International journal of environmental research and public health* 15(5) (2018); 1037.
46] F. Samari, H. Salehipoor, E. Eftekhar, & S. Yousefinejad, *New Journal of Chemistry*., 42(19) (2018); 15905-15916.
[47] J. Jalab, W. Abdelwahed, A. Kitaz, & R. Al-Kayali, *Heliyon*., 7(9) (2021).
[48] A.K. Mittal, Y. Chisti, & U.C. Banerjee, *Biotechnology advances*, 31(2) (20